ACS OMEGA

http://pubs.acs.org/journal/acsodf

Article

Magnetic Molecularly Imprinted Polymers Based on Dehydroabietylamine as Chiral Monomers for the Enantioseparation of *RS*-Mandelic Acid

Yidan Wang, Yande Chen, Congcong Li, Yi Zhu, Li Ge,* and Kedi Yang*

Cite This: *ACS Omega* 2021, 6, 14977−14984

Read Online

ACCESS | Metrics & More | Article Recommendations

ABSTRACT: Stereoselective adsorption of the enantiomers shows potential in the resolution of a racemate. In this work, we synthesized novel magnetic surface molecularly imprinted polymers (MIPs) on the surface of the γ-methacryloxypropyltrimethoxysilane (MPS)-modified Fe_3O_4@SiO_2 particles to utilize chiral dehydroabietylamine (DHA) as a functional monomer and *R*-mandelic acid as a template molecule (DHA-MIPs). We performed the resolution of mandelic acid racemate (*RS*-MA) via adsorption on the as-prepared MIPs. The results revealed that the MIPs have good affinity and high adsorption capacity for *R*-MA and show better enantioselective adsorption ability for *R*-MA than that for *S*-MA. One-stage adsorption of *RS*-MA on the MIPs can achieve up to 53.7% enantiomeric excess (ee) for *R*-MA. These help us to improve the chiral separation ability of the traditional MIPs using a chiral rather than an achiral monomer in MIP preparation. The MIPs can be employed as an economic and efficient adsorbent for chiral separation of MA racemate.

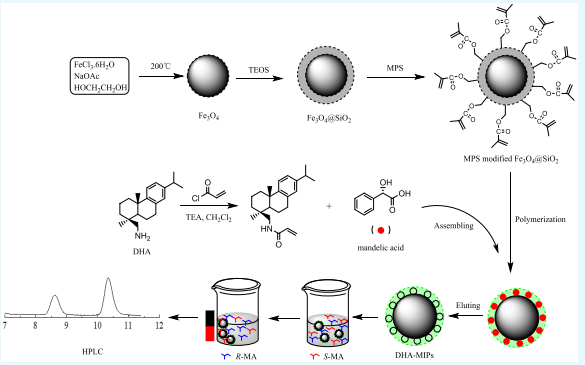

1. INTRODUCTION

The enantiomers of many chiral compounds often have marked differences in biological and therapeutic effects. Mostly, only one stereoisomer of the enantiomers has pharmacological activity, while the other may be inactive or, in worst cases, produce undesired or toxic effects. Thus, it is significant to obtain optically pure compounds by an economical and convenient method, but it is still a tough challenge because of the identical physical and chemical properties of enantiomers in an achiral environment. Currently, many resolution means have been developed for enantioseparation, including preferential crystallization, diastereomer crystallization, enantioselective extraction, and chiral high-performance liquid chromatography.[1] However, these methods have common shortcomings such as low efficiency, high cost, and poor versatile of enantiomers. Therefore, developing more efficient separation techniques of enantiomers is desired for obtaining pure enantiomers in the pharmaceutical industry to eliminate the unwanted isomer from racemate. Chiral adsorption offers several advantages over the other resolution methods, including low time cost, simplicity of operation, and easy scaling-up. This technique has attracted much attention for the chiral separation of racemic compounds.[2−6]

Molecular imprinting is a technique involving polymerization of functional monomers in the presence of template molecules. Removal of the templates from the polymers results in cavities and interaction sites within the polymers that are complementary to and have an affinity for the original template molecule. The common preparation methods of molecular imprinting include bulk polymerization, dispersion polymerization, surface imprinting, suspension polymerization, precipitation polymerization, emulsion polymerization, sol−gel technique, etc. The formed molecularly imprinted polymers (MIPs) as adsorption materials can selectively rebind the template and its structural analogues. MIPs have been applied to the chiral chromatographic stationary phases, chiral adsorbents, and other aspects.[4,7−12] However, despite its potential, almost all of the reported MIPs for the adsorption resolution of the racemate has focused on the fabrication by achiral and not chiral functional monomers in polymerization. The drawback is that the adsorption sites in the cavity of MIPs do not have enough enantiomeric discrimination ability, and they are not competent for selectively separating the enantiomers in most cases. To address this limitation, a few

Received: February 26, 2021
Accepted: May 24, 2021
Published: June 3, 2021

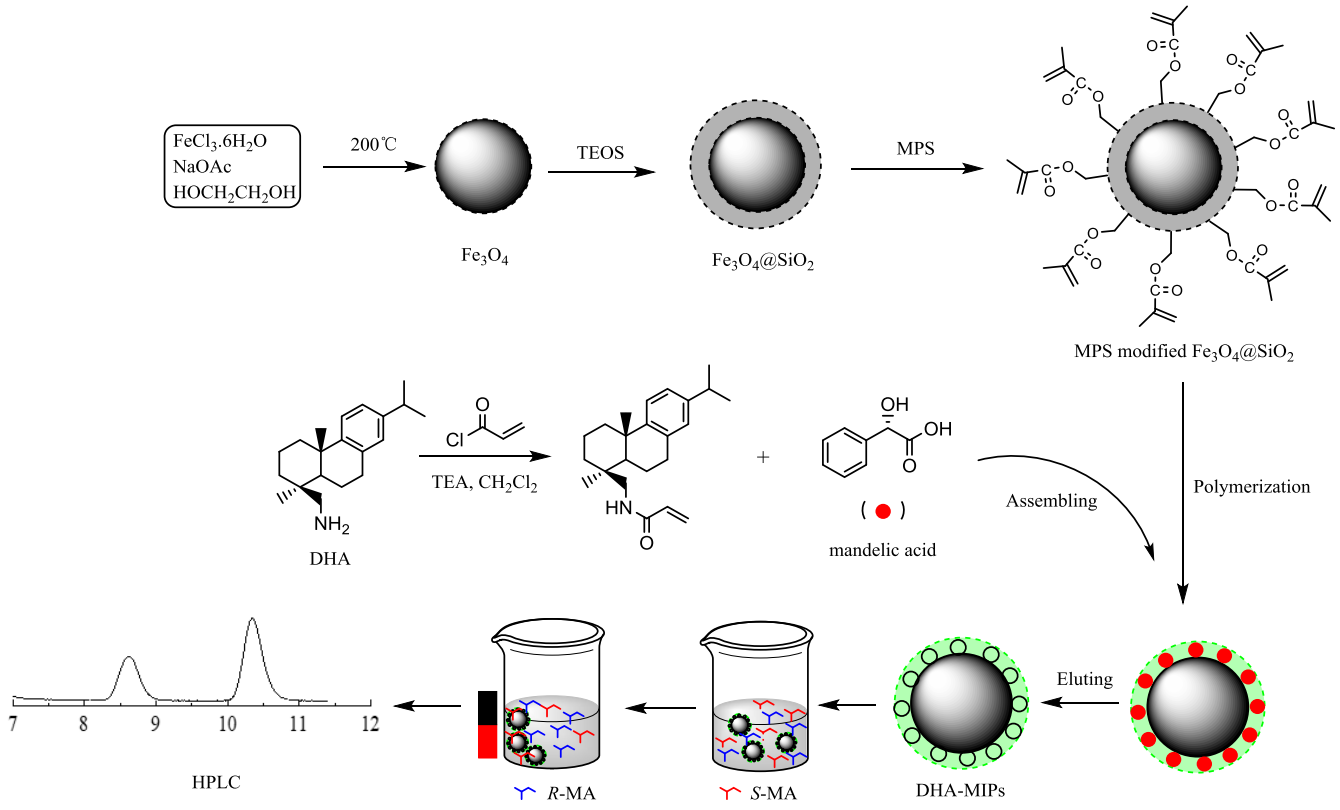

Figure 1. Schematic illustration of the preparation of DHA-MIPs and their enantioseparation of *RS*-MA.

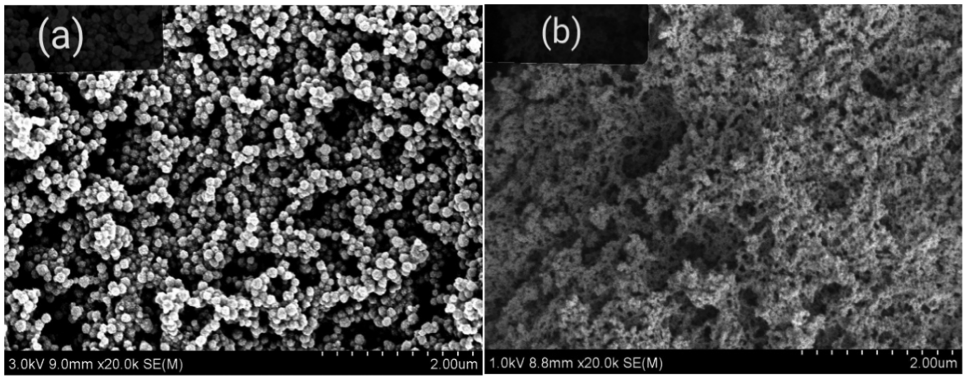

Figure 2. Scanning electron microscopy (SEM) images of (a) Fe_3O_4@SiO_2 and (b) DHA-MIPs.

studies of molecularly imprinted polymers based on chiral functional monomers have been investigated and reported.[13−18] As in this work, we aim to improve the enantioselective adsorption capacity of MIPs by employing an optically pure compound as a functional monomer to prepare the MIP adsorbent. Such modification is desirable because it may enhance the affinity and selectivity of MIPs, making it suitable for the resolution of enantiomers via adsorption.

Dehydroabietylamine (DHA), a natural optically pure compound, can be inexpensively obtained from commercial Amine D and has been used as a resolving agent for the separation of racemic carboxylic acids.[19−21] Additionally, the dehydroabietylamine derivatives also showed molecular recognition as chiral NMR solvating agents for some enantiomers.[22,23] In this work, dehydroabietylamine was used as a starting material to synthesize *N*-acryldehydroabietylamine and then the derivative was used as a chiral functional monomer to prepare the MIPs. Herein, we report the fabrication of DHA-based magnetic surface MIPs on the surface of Fe_3O_4@SiO_2 microspheres using *R*-mandelic acid (*R*-MA) as the template molecule and the chiral resolution of the racemic MA on these MIPs via adsorption.

2. RESULTS AND DISCUSSION

2.1. Synthesis and Characterization of DHA-MIP.

Figure 1 schematically presents the fabrication of DHA-MIPs using γ-methacryloxypropyltrimethoxysilane (MPS)-modified Fe_3O_4@SiO_2 and *N*-acryldehydroabietylamine. In this work, we employed the chiral molecule *N*-acryldehydroabietylamine as a monomer instead of achiral monomers in the conventional synthesis of MIPs and expected to improve the enantioselective interaction between the template molecule (*R*-MA) and monomers and the chiral recognition ability of the as-

https://doi.org/10.1021/acsomega.1c01054
ACS Omega 2021, 6, 14977−14984

synthesized DHA-MIPs for MA enantiomers. The typical morphologies of Fe_3O_4@SiO_2 particles and DHA-MIPs are shown in Figure 2. The prepared magnetite Fe_3O_4@SiO_2 particles are spherelike with a mean diameter of 120 nm and exhibit dispersibility (Figure 2a) but tend to clump and agglomerate due to polymerization during the preparation procedure of DHA-MIPs (Figure 2b). Thermogravimetric (TG) analysis (Figure 3) indicates that MPS-modified Fe_3O_4

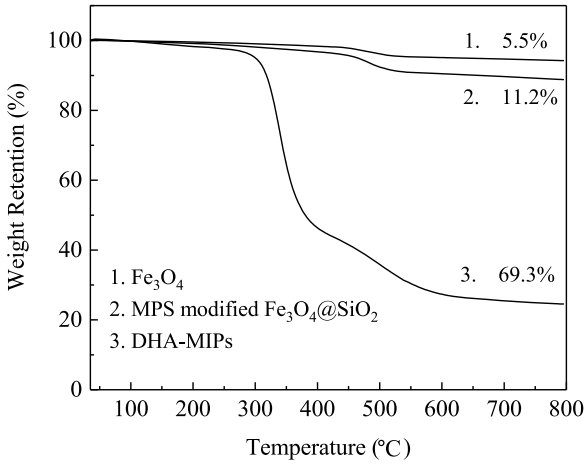

Figure 3. Thermogravimetric analysis curves of Fe_3O_4@SiO_2 and DHA-MIPs.

@SiO_2 has a weight loss of 11.2% when compared with the weight retention of bare Fe_3O_4 of 94.5%, which is probably ascribed to the decomposition of methacrylate layer on the particles. A higher mass loss for the DHA-MIPs (69.3 wt %) is mainly attributed to the thermal degradation of the organic polymer, indicating a thick imprinted layer on the Fe_3O_4@SiO_2 surface. Additionally, the magnetic properties of the prepared DHA-MIPs are measured with a vibrating sample magnetometer. The magnetic saturation (MS) values of the bare Fe_3O_4 particles and DHA-MIPs are 65 and 16 emu·g^{-1}, respectively. The lower MS of DHA-MIPs results from the nonmagnetic SiO_2 coatings and organic polymer layers, which increased the distance between magnetic particles. Even so, the prepared DHA-MIPs still possess a high magnetic response and can be easily isolated from the matrix conveniently by applying an external magnet (Figure 4, inset).

2.2. Adsorption of Template Molecules (*R*-MA) on the MIPs and Nonimprinted Polymers (NIPs). The absorption of *R*-MA on the DHA-based magnetic surface MIPs (denoted DHA-MIPs) and nonimprinted magnetic materials (denoted DHA-NIPs) at 30 °C were quantitatively evaluated by HPLC analysis, as shown in Figure 5. Although two types of materials have obvious adsorption, the DHA-MIPs exhibit a much higher adsorption capacity than DHA-NIPs due to the imprinting effect, which increases with increasing *R*-MA concentration. Further, the absorption behavior of *R*-MA on the two adsorbents is evaluated by the Langmuir equation (eq 1) and the Freundlich equation (eq 2).

$$1/Q_e = 1/Q_{max} + 1/K_L C_e \quad (1)$$

$$\ln Q_e = \ln K_F + n \ln C_e \quad (2)$$

where C_e is the equilibrium concentration, Q_e is the amount adsorbed at equilibrium, Q_{max} is the maximum adsorption

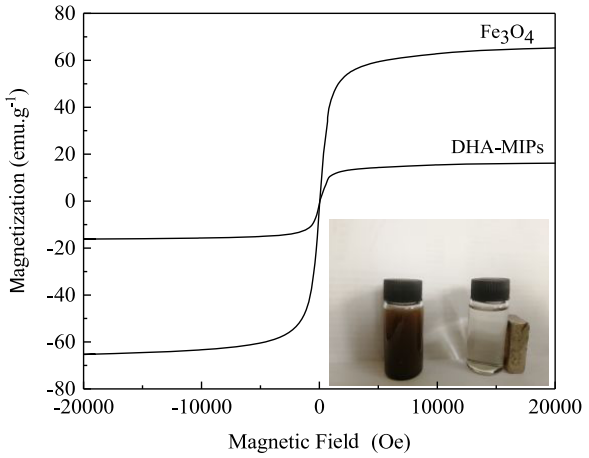

Figure 4. Magnetization curves of the prepared magnetic materials.

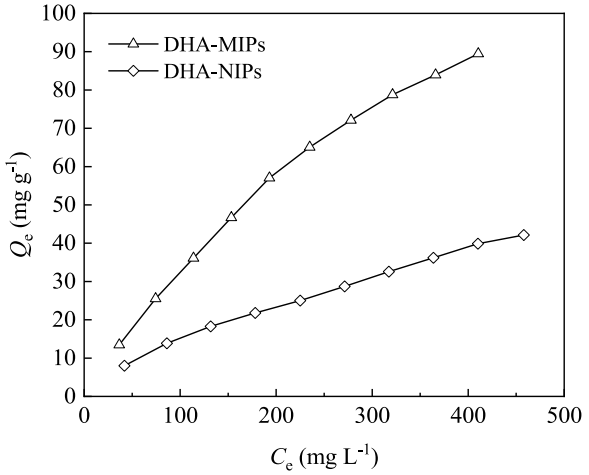

Figure 5. Isothermal adsorption equilibrium curves of *S*-MA on DHA-MIPs and DHA-NIPs.

capacity, K_L is the Langmuir constant, and K_F and n are Freundlich constants.

According to the fitted adsorption data (Table 1), the Langmuir equation fits better with the experimental data for

Table 1. Parameters of Langmuir and Freundlich Models

	Langmuir parameters			Freundlich parameters		
	Q_{max}	K_L	R^2	K_F	n	R^2
DHA-MIPs	207.90	0.39	0.9998	0.85	0.79	0.9931
DHA-NIPs	59.31	0.22	0.9935	0.63	0.68	0.9982

DHA-MIPs than the Freundlich equation, indicating that *R*-MA tends to monolayer adsorption on DHA-MIPs. The Freundlich model is suitable for depicting the adsorption behavior of DHA-NIPs, indicating multilayer adsorption of *R*-MA and the inhomogeneity of the adsorption site on the DHA-NIP surface. These results are in accord with the structure of DHA-MIPs and DHA-NIPs and demonstrate that MIPs possess better selective adsorption toward template molecules than NIPs.

Furthermore, the Scatchard model (eq 3) is also used to estimate the enantioselective adsorption properties of DHA-MIPs and DHA-NIPs.

https://doi.org/10.1021/acsomega.1c01054
ACS Omega 2021, 6, 14977−14984

$$Q_e/C_e = (Q_{max} - Q_e)/K \quad (3)$$

where Q_e is the equilibrium adsorption capacity of *R*-MA on DHA-MIPs or DHA-NIPs and Q_{max} is the apparent maximum adsorption capacity. C_e represents the *R*-MA concentration at adsorption equilibrium, and K is the dissociation constant. As seen in Figure 6, one fitted straight line is obtained for the

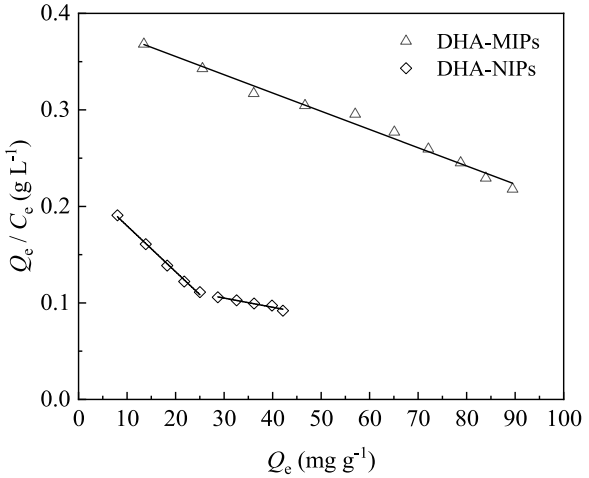

Figure 6. Scatchard plot analysis of the adsorption characteristics of DHA-MIPs and DHA-NIPs for *R*-MA.

adsorption of *R*-MA by DHA-MIPs but two lines by DHA-NIPs, which means that there are at least two different binding interaction sites in NIPs and but only one in DHA-MIPs.[24] These results indicate that DHA-MIPs possess higher chiral recognition to the *R*-MA template molecules than DHA-NIPs. The adsorption kinetics of *R*-MA (Figure 7) shows that the

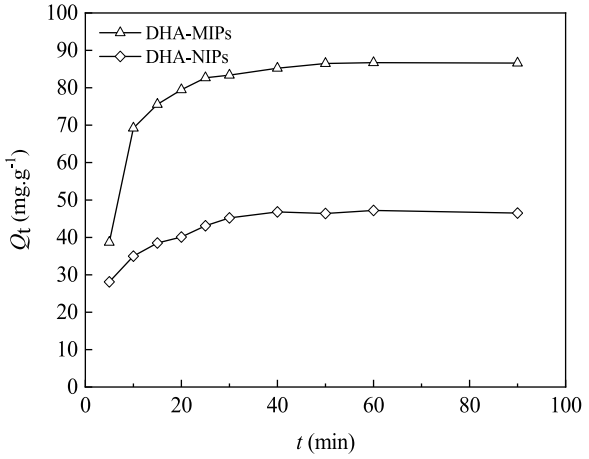

Figure 7. Adsorption kinetic curves of DHA-MIPs and DHA-NIPs for *R*-MA.

adsorption process quickly reached the thermodynamic equilibrium on the DHA-MIPs than that on the NIPs, indicating a lower internal diffusion resistance of template molecules in the polymer layer coated on Fe_3O_4@SiO_2 microspheres. By fitting the adsorption data via time, the adsorption of *R*-MA on both adsorbents can describe using the pseudo-second-order kinetic model (Figure 8 and Table 2).

2.3. Enantioselective Separation of RS-MA via Adsorption on the DHA-MIPs. The enantioselective

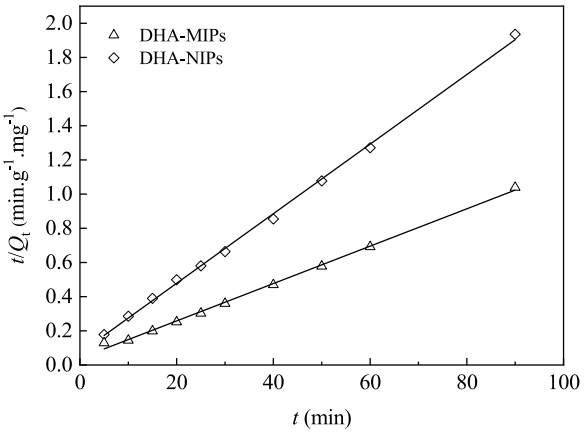

Figure 8. Kinetic model of pseudo-second-order for adsorption of *R*-MA on DHA-MIPs and DHA-NIPs.

Table 2. Second-Order Kinetic Parameters for Adsorption of *R*-MA on DHA-MIPs and DHA-NIPs[a]

	linear equations	k_2 (min·g^{-1}·mg^{-1})	R^2
MIPs	$t/Q_t = 0.039 + 0.011t$	0.28	0.9975
NIPs	$t/Q_t = 0.071 + 0.020t$	0.28	0.9986

[a]The pseudo-second-order equation is $t/Q_t = 1/k_2Q_e + t/Q_e$, where Q_e and Q_t are the adsorption capacities at equilibrium and at time t, respectively and k_2 is the rate constant of pseudo-second-order adsorption.

adsorption of *R*- and *S*-MA was explored by mechanically stirring DHA-MIP adsorbents with the racemic MA methanol solution at the desired concentration to reach an adsorption equilibrium. The enantioseparation results were measured by the adsorption capacity for *R*- and *S*-MA and the ee value for *R*-MA. As shown in Figure 9, the MIPs exhibit a higher

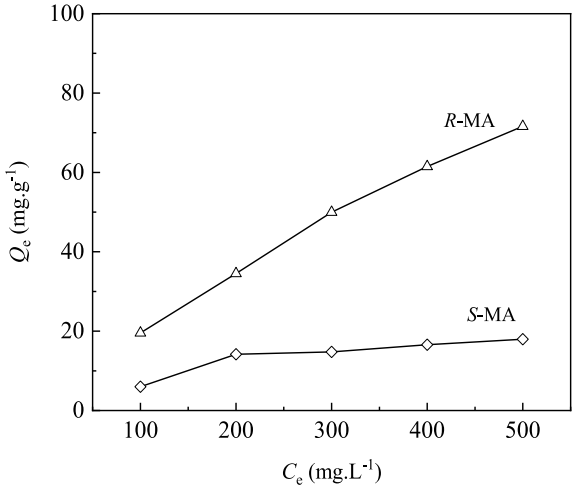

Figure 9. Chiral separation effect of *RS*-MA via DHA-MIP adsorption.

adsorption capacity for *R*-MA than that for *S*-MA in the same conditions. Also, the adsorption capacity for *R*-MA increases by increasing the MA concentration, but there is a slight change for *S*-MA. The DHA-MIPs demonstrate better selectivity toward *R*-MA owing to the stronger chiral interaction between MIPs and *R*-MA. At an initial concentration of MA methanol solution (500 mg·L^{-1}), one-stage

https://doi.org/10.1021/acsomega.1c01054
ACS Omega 2021, 6, 14977−14984

adsorption can yield an adsorption capacity of 71.63 mg·g^{-1} and up to 51.7% ee for *R*-MA. Besides, we assessed the effect of DHA-MIP amount on the resolution of racemic MA by adding a certain amount of DHA-MIPs (ranging from 20 to 200 mg) into 10 mL of 500 mg·L^{-1} *RS*-MA methanol solution at 30 °C. The relationship between the ee value and DHA-MIP amount is plotted in Figure 10. The results reveal there is an optimum

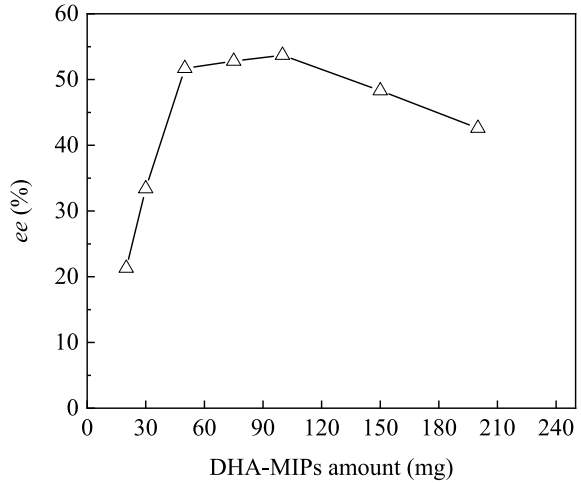

Figure 10. Effect of DHA-MIP amount on the ee value.

value of the DHA-MIP amount for a given amount of racemate. However, a downward trend in the ee value for *R*-MA was observed when the DHA-MIP amount exceeded 100 mg, which probably results from an increase of *S*-MA absorbed on the DHA-MIPs, but a nonobvious change of *R*-MA when increasing the DHA-MIP amount for a given amount of MA racemate.

Furthermore, the reusability of DHA-MIPs was investigated. DHA-MIPs (100 mg) were added to 10 mL of 500 mg·L^{-1} *RS*-MA methanol solution at 30 °C for enantioselective adsorption at equilibrium adsorption time. Afterward, the mixed solution of methanol/acetic acid (8:2, v/v) was applied to remove the adsorbed *R*- and *S*-MA. Finally, the obtained DHA-MIPs were used again for adsorption, and the above process was repeated 5 times. Figure 11 shows that the ee values slightly decreased

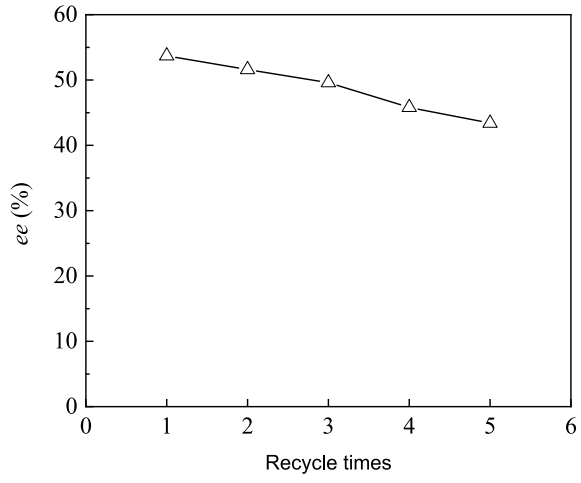

Figure 11. Reusability of DHA-MIPs for enantioselective adsorption of *RS*-MA.

as the number of recycle times increased. It can be seen that after five cycles, the ee value for *R*-MA still reaches 43.4%, which demonstrates that the DHA-MIPs have good reusability.

2.4. Comparison with Other Enantioseparation Methods for *RS*-MA. *R*-MA is an intermediate or chiral synthon for the synthesis of penicillin, cephalosporin, and antitumor agents.[25] Some approaches have been developed for the enantioseparation of *RS*-MA to obtain *R*-MA.[26−33] However, it is still challenging to design an easily prepared, economical, and efficient chiral material or separation medium used for the enantiomer resolution of MA. He[34] reported the separation of *RS*-MA on the MIPs prepared by utilizing achiral methacrylic acid as the monomer and *S*-MA as the molecule template and achieved only 30.2% ee. Compared to our result of 53.7% ee, it is proved that the MIPs prepared by employing the chiral monomer can markedly improve the enantioselective adsorption ability for *R*-MA. Deng[35] conducted the resolution of MA racemate using *β*-CD-modified Fe_3O_4@SiO_2/Au as adsorbents and obtained 63.5% ee. However, the preparation procedure of this adsorption material is intricate. In Table 3,

Table 3. Comparison with the Other Reported Enantioseparation Methods of *RS*-MA

resolution method	separation media	resolution effect (% ee)	ref
chiral extraction	D-(+)-DTTA/*β*-CD derivatives	20.9	25
chiral extraction	Cu(II)-*β*-CD/tritonX-114	67.9	36
chiral extraction	poly(MAH-*β*-CD-*co*-NIPAAm)	11.8	28
chiral extraction	chiral diphosphine ligands	50.6	33
		45.5	37
chiral extraction	chiral ionic liquid based on L-proline	17.4	38
chiral adsorption	MAA-MIPs of *S*-MA	30.2	34
chiral adsorption	Fe_3O_4@SiO_2/Au/*β*-CD	63.5	35
chiral adsorption	nautilus-E@antibiotic eremomycin	51.1	31
chiral adsorption	DHA-MIPs of *R*-MA	53.7	this work

we compare the separation effect of *RS*-MA based on DHA-MIP adsorption with the previously published experimental data by chiral extraction and adsorption. DHA-MIPs showed better resolution of *RS*-MA than most of the reported chiral separation media. Also, the DHA-MIPs have some competitive advantages, such as facile fabrication and no toxic chemicals during synthesis. Furthermore, these help to improve the chiral separation ability of the traditional MIPs using a chiral monomer rather than an achiral one in MIP preparation.

2.5. Chiral Recognition Analysis of DHA-MIPs. To understand the enantiomer recognition of DHA-MIPs to *R*- and *S*-MA, we used ^{1}H NMR experiments to evaluate the diastereomeric interaction between DHA functional monomers and MA enantiomers by the chemical shift changes of the chiral proton **1** of the MA molecule (see Figure 12). From Figure 12, it is observed that the chemical shift of proton changes obviously and, especially, the peak of proton splits from singlet to doublet, which indicates that there are different interactions between DHA and *R*- or *S*-enantiomer, such as hydrogen-bonding, *π*−*π*, and van der Waals interactions,

https://doi.org/10.1021/acsomega.1c01054
ACS Omega 2021, 6, 14977−14984

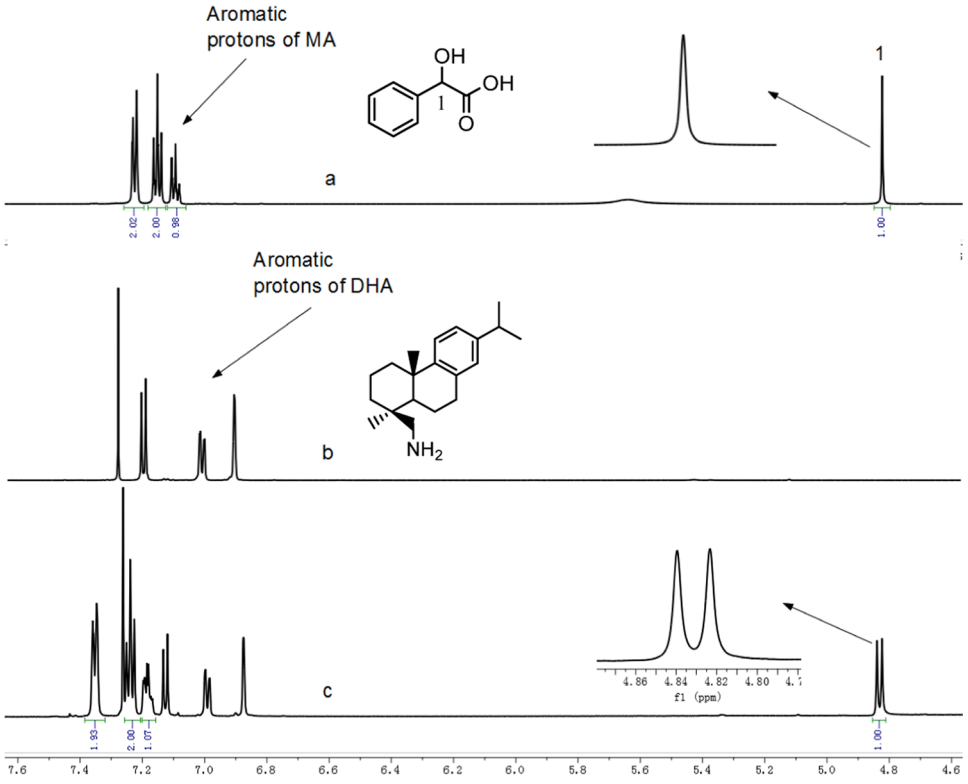

Figure 12. ^{1}H NMR (600MHz, CD_3Cl) spectra of (a) MA, (b) DHA, and (c) MA/DHA complex.

illustrating that the complexes of DHA/*R*-MA and DHA/*S*-MA formed are diastereoisomers and then proton **1** of *R*- and *S*-MA in the complexes is not equivalent. A difference in the shift of ca. 0.016 ppm between *R*-MA and *S*-MA is observed. These results demonstrates the chiral recognition of DHA toward *R*-MA and *S*-MA. Based on the molecular structures of DHA and MA, the interactions, mainly including hydrogen-bonding and $\pi-\pi$ stacking interactions between DHA and MA, may be responsible for chiral discrimination. Additionally, we estimated the binding energy between the optimized conformations of DHA and *R*- or *S*-MA by the DFT method (B3LYP-D3/6-31G+(d,p)). The binding energies of the DHA/*R*- and *S*-MA complexes are −0.032 and −0.027 Hartree, respectively, revealing that DHA/*R*-MA is more stable than DHA/*S*-MA and DHA can selectively recognize *R*-MA. The DHA-MIPs prepared with chiral DHA monomers have the imprinting cavities to match with the template molecules of *R*-MA; in addition, the chiral recognition sites in the cavities make the interaction much stronger between *R*-MA and MIPs. This double response enhances the diastereomeric interactions between DHA-MIPs and *R*-MA to form more stable complexes. Thus, the chiral resolution of MA via adsorption was achieved based on the interaction difference of *R*-MA and *S*-MA with DHA-MIPs.

3. CONCLUSIONS

In summary, we have synthesized the DHA-MIPs with enantioselective recognition ability via copolymerization of *N*-acryldehydroabietylamine and EGDMA on the surface of the MPS-modified Fe_3O_4@SiO_2 microspheres by employing *R*-MA as a template molecule. These DHA-MIPs were successfully applied to the separation of MA racemate by an adsorption method. The results revealed that the DHA-MIPs possessed better affinity and selectivity for *R*-MA than those for *S*-MA and showed a higher adsorption capacity and ee value for *R*-MA. Using the one-stage adsorption of *RS*-MA on the DHA-MIPs, up to 53.7% ee for *R*-MA can be achieved. Based on our experimental results, the as-synthesized DHA-MIPs can be used as effective adsorbents for the chiral separation of *RS*-MA. Also, they have the potential for the adsorption resolution of other racemates.

4. EXPERIMENTAL SECTION

4.1. Materials. Optically pure (+)-dehydroabietylamine (mass fraction higher than 95%, supplied by Wuhan Yuancheng Gongchuang Technology Co., Ltd., China) was directly used without further purification. γ-Methacryloxypropyltrimethoxysilane (MPS, 95%), ethylene glycol dimethacrylate (EGDMA, 95%), tetraethoxysilane (TEOS), poly(vinylpyrrolidone) (PVP, 98%), and 2,2-azobisisobutyronitrile (AIBN) were purchased from Shanghai Macklin Biochemical Co., Ltd. *RS*-mandelic acid (MA), *R*-MA, and *S*-MA were purchased from Adamas Chemistry Co., Ltd. The other chemicals and solvents used in this study were of analytical grade.

4.2. Synthesis of *N*-Acryldehydroabietylamine. *N*-Acryldehydroabietylamine was prepared according to the procedure described by Laaksonen.[22] About 3.75 g of dehydroabietylamine (10 mmol) and 3.0 mL of triethylamine were dissolved in 20 mL of CH_2Cl_2, and then, 10 mmol acryloyl chloride in 10 mL of CH_2Cl_2 was dropped into the solution at −5 °C under stirring. Then, the mixture was stirred at room temperature for another 12 h in a N_2 atmosphere. The resulting mixture was washed successively with dilute hydrochloric acid, saturated K_2CO_3 solution, and distilled water. After evaporation of the solvent under reduced pressure, the residue was purified on silica-gel column chromatography through gradient elution using ethyl acetate and methanol.

https://doi.org/10.1021/acsomega.1c01054
ACS Omega 2021, 6, 14977−14984

Light yellow, solid *N*-acryldehydroabietylamine (75.2% yield) was obtained by evaporating the solvent.

4.3. Preparation of the MPS-Modified Fe_3O_4@SiO_2 Microspheres. The Fe_3O_4 microspheres were synthesized according to the method reported by Liu[39] with some modifications. A total of 5 mmol $FeCl_3{\cdot}6H_2O$, 47 mmol sodium acetate, 1.4 mmol sodium citrate, and 0.4 g of PVP were dissolved in 60 mL of glycol to form a reddish-brown transparent solution by stirring. Then, the solution was transferred to a 100 mL Teflon-lined stainless steel autoclave and reacted at 200 °C for 24 h. After cooling down to room temperature, the synthesized Fe_3O_4 particles were collected by a magnet, washed with deionized water and ethanol in turn, and dried in a vacuum oven at 60 °C for 12 h. The Fe_3O_4@SiO_2 microspheres were prepared using the hydrolysis method proposed by Stöber.[40] Typically, 5 g of Fe_3O_4 particles was dispersed to form a suspension by sonicating for 30 min in a solution consisting of 400 mL of ethanol, 100 mL of deionized water, and 10 mL of TEOS. Ammonia aqueous solution (20 mL, 25 wt %) was dropped into the suspension, and the mixture was stirred at room temperature for 12 h. The obtained Fe_3O_4@SiO_2 was collected by a magnet, washed with ethanol and deionized water several times, and then dried under vacuum at 60 °C. Then, 4 g of Fe_3O_4@SiO_2 microspheres was dispersed in 800 mL of toluene, and 20 mL of MPS was added. After stirring the mixture overnight at 110 °C under a N_2 atmosphere, the Fe_3O_4@SiO_2 microspheres modified with MPS were collected by an external magnet and rinsed with ethanol and water.

4.4. Fabrication of the DHA-Based Magnetic Surface MIPs and NIPs. MPS-modified Fe_3O_4@SiO_2 microspheres (5.0 g) were dispersed in a mixture of 5.0 mmol *R*-MA, 20 mmol *N*-acryldehydroabietylamine, and 150 mL of toluene. This suspension was first preassembled for 6 h at room temperature. Subsequently, 100 mmol EGDMA and 1.25 g of AIBN were added to initiate the polymerization at 65 °C over 24 h under a N_2 atmosphere and then DHA-MIPs were obtained. For comparison, DHA-NIPs were prepared by the same procedure in the absence of the template molecules of *R*-MA. Both MIPs and NIPs were washed with methanol/acetic acid (8:2, v/v) and methanol alternately to remove the template molecules and the unreacted monomers before use.

4.5. Adsorption Experiments. Fifty milligrams of DHA-MIPs or DHA-NIPs was added into a 25 mL conical flask containing 10 mL of *R*-MA or *RS*-MA methanol solution at the desired concentration (0.05−0.5 $mg{\cdot}mL^{-1}$, pH = 7.0). The flask was shaken at 30 °C using a thermostatic water bath shaker. After achieving adsorption equilibrium, the adsorbents were separated by an external magnet, and the supernatant was analyzed to determine the residual concentration of *S*-MA and *R*-MA in methanol solution by chiral HPLC. The absorption capacity (Q_e, $mg{\cdot}g^{-1}$) of DHA-MIPs or DHA-NIPs for MA was calculated by eq 4.

$$Q_e = (C_0 - C_e) \times V/m \tag{4}$$

where V is the solution volume and m is the mass of the adsorbent, and C_0 and C_e are the initial and equilibrium concentrations of *S*-MA or *R*-MA in solution, respectively.

For the adsorption resolution of MA enantiomers on the DHA-MIPs, the effects of enantioselective separation evaluated by the enantiomeric excess value (ee) were calculated according to eq 5.

$$\text{ee}\,\% = (C_R - C_S)/(C_R + C_S) \times 100 \tag{5}$$

where C_R and C_S represent the concentrations of *R*-MA and *S*-MA in the supernatant after adsorption, respectively.

4.6. Chiral Chromatographic Conditions. The analysis of *S*-MA and *R*-MA was performed on a Phenomenex chiral MD(2) column (250 mm × 4.6 mm, 5.0 μm). A mixture of *n*-hexane and isopropanol in an 80:20 volume ratio (containing 0.1% TFA) was employed as a mobile phase at a flow rate of 1.0 $mL{\cdot}min^{-1}$. The UV detection wavelength was set at 230 nm.

4.7. Computational Methods. All theoretical calculations were carried out with the program of Gaussian 16 package.[41] The geometry structure optimization of DHA, *R*- or *S*-MA, and their complexes and the binding energy calculations between the optimized conformations of DHA and *R*- or *S*-MA were performed by the density functional theory (DFT) method at the level of B3LYP-D3/6-31G+(d,p). The binding energy (E_{bind}) was calculated according to eq 6

$$E_{bind} = E_{com} - (E_a + E_b) \tag{6}$$

where E_{com}, E_a, and E_b are the total energies of complexes, DHA, and *R*- or *S*-MA, respectively.

AUTHOR INFORMATION

Corresponding Authors

Li Ge − *Department of Pharmaceutical Engineering, Medical College, Guangxi University, Nanning 530004, China*; Email: geli_2009@163.com

Kedi Yang − *Department of Pharmaceutical Engineering, Medical College, Guangxi University, Nanning 530004, China*; orcid.org/0000-0002-2195-8782; Email: kdyang@163.com

Authors

Yidan Wang − *School of Chemistry & Chemical Engineering, Guangxi University, Nanning 530004, China*

Yande Chen − *School of Chemistry & Chemical Engineering, Guangxi University, Nanning 530004, China*

Congcong Li − *School of Chemistry & Chemical Engineering, Guangxi University, Nanning 530004, China*

Yi Zhu − *School of Chemistry & Chemical Engineering, Guangxi University, Nanning 530004, China*

Complete contact information is available at: https://pubs.acs.org/10.1021/acsomega.1c01054

Notes

The authors declare no competing financial interest.

ACKNOWLEDGMENTS

This work was financially supported by the National Natural Science Foundation of China (NSFC, Grant No. 21666003).

REFERENCES

(1) Ahuja, S. *Chiral Separation Methods for Pharmaceutical and Biotechnological Products*; Wiley Online Library, 2011.

(2) Duri, S.; Tran, C. D. Enantiomeric selective adsorption of amino acid by polysaccharide composite materials. *Langmuir* **2014**, *30*, 642−650.

(3) He, K.; Qiu, F.; Qin, J.; Yan, J.; Yang, D. Preparation and characterization of L-phenylalanine-derivatized β-cyclodextrin-bonded silica and its application on chiral separation of alanine acid racemates. *Korean J. Chem. Eng.* **2013**, *30*, 2078−2087.

(4) Su, M.-X.; Liu, Z.-Y.; Chen, J.-L.; Cheng, L.-F.; Li, B.; Yan, F.; Di, B. Stereoselective adsorption utilizing L-phenylalanine imprinting chiral ordered mesoporous silica. *RSC Adv.* **2014**, *4*, 54998−55002.
(5) Vulugundam, G.; Misra, S. K.; Ostadhossein, F.; Schwartz-Duval, A. S.; Daza, E. A.; Pan, D. (−)/(+)-Sparteine induced chirally-active carbon nanoparticles for enantioselective separation of racemic mixtures. *Chem. Commun.* **2016**, *52*, 7513−7516.
(6) Zhu, W.; Wang, Q.; Du, K.; Yao, S.; Song, H. Fabrication and characterization of novel tentacle-type adsorbent for resolution of chiral drugs. *Chin. Sci. Bull.* **2013**, *58*, 3390−3397.
(7) Kempe, M.; Mosbach, K. Molecular imprinting used for chiral separations. *J. Chromatogr. A* **1995**, *694*, 3−13.
(8) Paik, P.; Gedanken, A.; Mastai, Y. Chiral-mesoporous-polypyrrole nanoparticles: Its chiral recognition abilities and use in enantioselective separation. *J. Mater. Chem.* **2010**, *20*, 4085−4093.
(9) Ansell, R. J.; Kuah, J. K.; Wang, D.; Jackson, C. E.; Bartle, K. D.; Clifford, A. A. Imprinted polymers for chiral resolution of (±)-ephedrine, 4: Packed column supercritical fluid chromatography using molecularly imprinted chiral stationary phases. *J. Chromatogr. A* **2012**, *1264*, 117−123.
(10) Gabashvili, A.; Medina, D. D.; Gedanken, A.; Mastai, Y. Templating mesoporous silica with chiral block copolymers and its application for enantioselective separation. *J. Phys. Chem. B* **2007**, *111*, 11105−11110.
(11) Paik, P.; Gedanken, A.; Mastai, Y. Enantioselective separation using chiral mesoporous spherical silica prepared by templating of chiral block copolymers. *ACS Appl. Mater. Interfaces* **2009**, *1*, 1834−1842.
(12) Yang, Z.; Shan, Y.-L.; Yu, B.; Gao, Q.; Cong, H.-L. Selective adsorption of chiral mandelic acid by molecularly imprinted poly (dimethylaminoethyl methacrylate) on surface of magnetic silica microspheres. *Integr. Ferroelectr.* **2017**, *180*, 133−138.
(13) Jiang, J.; Song, K.; Chen, Z.; Zhou, Q.; Tang, Y.; Gu, F.; Zuo, X.; Xu, Z. Novel molecularly imprinted microsphere using a single chiral monomer and chirality-matching (*S*)-ketoprofen template. *J. Chromatogr. A* **2011**, *1218*, 3763−3770.
(14) Zhou, Q.; He, J.; Tang, Y.; Xu, Z.; He, L.; Kang, C.; Jiang, J. A novel hydroquinidine imprinted microsphere using a chirality-matching N-acryloyl-L-phenylalanine monomer for recognition of cinchona alkaloids. *J. Chromatogr. A* **2012**, *1238*, 60−67.
(15) Akgönüllü, S.; Yavuz, H.; Denizli, A. Preparation of imprinted cryogel cartridge for chiral separation of l-phenylalanine. *Artif. Cells, Nanomed., Biotechnol.* **2017**, *45*, 800−807.
(16) Alizadeh, T.; Bagherzadeh, A.; Shamkhali, A. N. Synthesis of nano-sized stereoselective imprinted polymer by copolymerization of (S)-2-(acrylamido) propanoic acid and ethylene glycol dimethacrylate in the presence of racemic propranolol and copper ion. *Mater. Sci. Eng., C* **2016**, *63*, 247−255.
(17) Knutsson, M.; Andersson, H. S.; Nicholls, I. A. Novel chiral recognition elements for molecularly imprinted polymer preparation. *J. Mol. Recognit.* **1998**, *11*, 87−90.
(18) Wang, L.; She, X.; Chen, Z.; et al. Preparation and characterization of a chiral molecularly imprinted polymer with a novel functional monomer for controlled release of *S*-sulpiride. *Int. J. Pharm.* **2021**, *601*, No. 120526.
(19) Gottstein, W. J.; Cheney, L. C. Dehydroabie tylamine. A New Resolving Agent1. *J. Org. Chem.* **1965**, *30*, 2072−2073.
(20) Bolchi, C.; Fumagalli, L.; Moroni, B.; Pallavicini, M.; Valoti, E. A short entry to enantiopure 2-substituted 1,4-benzodioxanes by efficient resolution methods. *Tetrahedron: Asymmetry* **2003**, *14*, 3779−3785.
(21) Bolchi, C.; Pallavicini, M.; Fumagalli, L.; Rusconi, C.; Binda, M.; Valoti, E. Resolution of 2-substituted 1,4-benzodioxanes by entrainment. *Tetrahedron: Asymmetry* **2007**, *18*, 1038−1041.
(22) Laaksonen, T.; Heikkinen, S.; Wahala, K. Synthesis and applications of secondary amine derivatives of (+)-dehydroabietylamine in chiral molecular recognition. *Org. Biomol. Chem.* **2015**, *13*, 10548−10555.
(23) Foreiter, M. B.; Gunaratne, H. Q. N.; Nockemann, P.; Seddon, K. R.; Stevenson, P. J.; Wassell, D. F. Chiral thiouronium salts: synthesis, characterisation and application in NMR enantio-discrimination of chiral oxoanions. *New. J. Chem.* **2013**, *37*, 515−533.
(24) Lv, Y.-K.; Ma, Y.; Zhao, X.-B.; Jia, C.-L.; Sun, H.-W. Grafting of norfloxacin imprinted polymeric membranes on silica surface for the selective solid-phase extraction of fluoroquinolones in fish samples. *Talanta* **2012**, *89*, 270−275.
(25) Tang, K.; Yi, J.; Huang, K.; Zhang, G. Biphasic recognition chiral extraction: a novel method for separation of mandelic acid enantiomers. *Chirality* **2009**, *21*, 390−395.
(26) De Klerck, K.; Mangelings, D.; Vander Heyden, Y. Supercritical fluid chromatography for the enantioseparation of pharmaceuticals. *J. Pharm. Biomed. Anal.* **2012**, *69*, 77−92.
(27) Tarigh, G. D.; Shemirani, F. In situ immobilization of a general resolving agent on the magnetic multi-wall carbon nanotube for the direct enantioenrichment of DL-mandelic acid. *Talanta* **2015**, *144*, 899−907.
(28) Tan, Z.; Li, F.; Zhao, C.; Teng, Y.; Liu, Y. Chiral separation of mandelic acid enantiomers using an aqueous two-phase system based on a thermo-sensitive polymer and dextran. *Sep. Purif. Technol.* **2017**, *172*, 382−387.
(29) Fu, Y.; Wang, L.; Chen, Q.; Zhou, J. Enantioselective recognition of chiral mandelic acid in the presence of Zn(II) ions by l-cysteine-modified electrode. *Sens. Actuators, B* **2011**, *155*, 140−144.
(30) Li, H.; Huang, Q.; Li, D.; Li, S.; Wu, X.; Wen, L.; Ban, C. Generation of a Molecular Imprinted Membrane by Coating Cellulose Acetate onto a ZrO2-Modified Alumina Membrane for the Chiral Separation of Mandelic Acid Enantiomers. *Org. Process Res. Dev.* **2018**, *22*, 278−285.
(31) Reshetova, E.; Gogolishvili, O. Adsorption of mandelic acid enantiomers on a chiral stationary phase with a grafted antibiotic eremomycin. *J. Liq. Chromatogr. Relat. Technol.* **2018**, *41*, 561−571.
(32) Deng, X.; Li, W.; Ding, G.; Chen, X. Enantioselective separation of RS-mandelic acid using *β*-cyclodextrin modified Fe 3 O 4@ SiO 2/Au microspheres. *Analyst* **2018**, *143*, 2665−2673.
(33) Liu, X.; Ma, Y.; Liu, Q.; Wei, X.; Yang, J.; Yu, L. Chiral extraction of amino acid and mandelic acid enantiomers using chiral diphosphine ligands with tunable dihedral angles. *Sep. Purif. Technol.* **2019**, *221*, 159−165.
(34) He, X. R. Preparation of surface imprinted material of chiral drug mandelic acid and study on its recognition and chiral enantioseparation property. Master, North University of China, 2017.
(35) Deng, X.; Li, W.; Ding, G.; Chen, X. Enantioselective separation of RS-mandelic acid using beta-cyclodextrin modified Fe_3O_4@SiO_2/Au microspheres. *Analyst* **2018**, *143*, 2665−2673.
(36) Xing, J.-M.; Li, F.-F. Chiral separation of mandelic acid by temperature-induced aqueous two-phase system. *J. Chem. Technol. Biotechnol.* **2012**, *87*, 346−350.
(37) Ma, Y.; Liu, X.; Zhou, W.; Cao, T. Enantioselective liquid-liquid extraction of DL-mandelic acid using chiral diphosphine ligands as extractants. *Chirality* **2019**, *31*, 248−255.
(38) e Silva, F. A.; Kholany, M.; Sintra, T. E.; Caban, M.; Stepnowski, P.; Ventura, S. P. M.; Coutinho, J. A. P. Aqueous Biphasic Systems Using Chiral Ionic Liquids for the Enantioseparation of Mandelic Acid Enantiomers. *Solvent Extr. Ion Exch.* **2018**, *36*, 617−631.
(39) Liu, Y.; Li, C.; Zhang, H.; Fan, X.; Liu, Y.; Zhang, Q. One-pot hydrothermal synthesis of highly monodisperse water-dispersible hollow magnetic microspheres and construction of photonic crystals. *Chem. Eng. J.* **2015**, *259*, 779−786.
(40) Stöber, W.; Fink, A.; Bohn, E. Controlled growth of monodisperse silica spheres in the micron size range. *J. Colloid Interface Sci.* **1968**, *26*, 62−69.
(41) Frisch, M. J.; Trucks, G. W.; Schlegel, H. B. et al. *Gaussian 16*, revision C.01; Gaussian, Inc.: Wallingford, CT, 2019.

https://doi.org/10.1021/acsomega.1c01054
ACS Omega 2021, 6, 14977−14984